·Neuroimaging Study of Alzheimer's Disease·

^{11}C-PIB PET and ^{18}F-FDG PET in patients with Alzheimer's disease and amnestic mild cognitive impairment

^{11}C-PIB PET和^{18}F-FDG PET显像诊断阿尔茨海默病与遗忘型轻度认知损害的临床价值

Shi Zhihong[1,2], Wang Ying[3], Liu Shuai[1,2], Liu Shuling[1,2], Zhou Yuying[1,2], Wang Jinhuan[1,4], Cai Li[3], Gao Shuo[3], Ji Yong[1,2]

[1]Tianjin Key Laboratory of Cerebrovascular and Neurodegenerative Diseases, Tianjin 300060, China

[2]Department of Neurology, Tianjin Huanhu Hospital, Tianjin 300060, China

[3]PET-CT Center, Tianjin Medical University General Hospital, Tianjin 300052, China

[4]Department of Neurosurgery, Tianjin Huanhu Hospital, Tianjin 300060, China

Keywords

Alzheimer disease; Cognition disorders; Apolipoprotein E4; Radioactive tracers; Positron-emission tomography.

【关键词】 阿尔茨海默病；认知障碍；载脂蛋白E4；放射性示踪剂；正电子发射断层显像术

Correspondence

Ji Yong, M.D., Ph.D.
Tianjin Huanhu Hospital
Qixiangtai Road 122, Hexi District
Tianjin 300060, China
Email: jiyongusa@126.com

Received: 8 November, 2013.

doi:10.3969/j.issn.1672-6731.2014.03.013

Shi Zhihong and Wang Ying contributed equally to this work.

Abstract

Objective The present study investigated the relationship between amyloid deposition and glucose metabolism using Pittsburgh compound B (^{11}C - PIB) and fluorodeoxyglucose (^{18}F - FDG) positron - emission tomography (PET) in patients with Alzheimer's disease (AD) and amnestic mild cognitive impairment (aMCI) and assessed the apolipoprotein E (*ApoE*) *ε4* allele to explore the correlation between aMCI and AD. **Methods** Amyloid load in the brain and cerebral glucose metabolism were determined and *ApoE* genotypes were analyzed in patients with AD (N = 14), aMCI (N = 10), and healthy controls (N = 5). **Results** The mean ^{11}C-PIB standardized uptake value ratio (SUVR) was higher in inferior parietal lobe, lateral temporal cortex, frontal cortex, posterior cingulate cortex and precuneus, occipital lobe, and striatum in AD patients compared with controls ($P < 0.05$). ^{11}C-PIB binding levels in aMCI patients were bimodal. No significant difference in the ^{11}C - PIB SUVR was found between the ^{11}C - PIB + aMCI subgroup and AD group ($P > 0.05$). ^{18}F - FDG PET revealed hypometabolism in bilateral parietal lobes, temporal lobe, and precuneus in 3 of 5 ^{11}C - PIB + aMCI subjects, including two of them with *ApoE ε 4* allele converted to AD, and hypometabolism in the bilateral frontal lobe and anterior cingulate in 3 of 5 ^{11}C-PIB - aMCI subjects. **Conclusions** ^{11}C-PIB PET is a powerful tool for screening aMCI with AD pathology. The aMCI patients with AD pathology who presented hypometabolism in the parietal lobe, lateral temporal cortex, precuneus and with *ApoE ε 4* allele are more likely to convert to clinical AD dementia.

【摘要】 目的 应用^{11}C-PIB PET和^{18}F-FDG PET显像研究阿尔茨海默病和遗忘型轻度认知损害患者β-淀粉样蛋白（Aβ）沉积与葡萄糖代谢之间的关系，联合载脂蛋白E（*ApoE*）基因型进一步探讨遗忘型轻度认知损害与阿尔茨海默病的相关性。**方法** 利用PET显像对阿尔茨海默病（14例）、遗忘型轻度认知损害（10例）和正常对照者（5例）脑组织Aβ沉积和葡萄糖代谢变化进行分析，采用聚合酶链反应-限制性片段长度多态性方法对*ApoE*基因型进行分析。**结果** 阿尔

茨海默病组患者^{11}C-PIB标准化摄取比值在下顶叶、颞叶外侧、额叶、后扣带回皮质和楔前叶、枕叶和纹状体均高于正常对照组($P<0.05$)；遗忘型轻度认知损害组患者脑组织^{11}C-PIB结合水平呈双峰形。^{11}C-PIB+aMCI亚组与阿尔茨海默病组、^{11}C-PIB–aMCI亚组与正常对照组之间^{11}C-PIB标准化摄取比值差异均无统计学意义($P>0.05$)。^{18}F-FDG PET显像显示，3/5例^{11}C-PIB+aMCI亚组患者双侧顶叶、颞叶和楔前叶代谢减低，其中2例*ApoEε4*等位基因携带者随访期间进展至阿尔茨海默病；3/5例^{11}C-PIB–aMCI亚组患者双侧额叶和前扣带回代谢减低。**结论** ^{11}C-PIB PET显像是筛查具有阿尔茨海默病病理特点的遗忘型轻度认知损害患者的有效工具。具有阿尔茨海默病病理特征的遗忘型轻度认知损害患者可伴有顶叶、颞叶外侧皮质和楔前叶代谢减低，其中*ApoEε4*等位基因携带者更易进展至阿尔茨海默病痴呆。

Introduction

Alzheimer's disease (AD) is an age - related neurodegenerative disorder that results in a progressive loss of cognitive function. It is characterized by the accumulation of amyloid-beta (Aβ) peptide into amyloid plaques in extracellular brain parenchyma and intraneuronal neurofibrillary tangles (NFTs) caused by the abnormal phosphorylation of tau protein [1]. Amyloid deposits and tangles are necessary for the postmortem diagnosis of AD [2].

Positron - emission tomography with ^{18}F - fluorodeoxyglucose (^{18}F - FDG PET) highlights the differential distribution of pathology in dementing disorders and has been used to study neurodegenerative diseases for over two decades. AD causes hypometabolism predominantly in posterior regions, including posterior temporoparietal association cortex and posterior cingulate cortex [3]. Frontotemporal dementia (FTD) causes hypometabolism predominantly in anterior regions, including frontal lobes, anterior temporal cortex and anterior cingulate cortex [4]. ^{18}F-FDG PET studies with small samples of patients with mild cognitive impairment (MCI) showed that parietotemporal and posterior cingulate hypometabolism may characterize patients who later convert to AD [5 - 6]. Brain FDG retention is a nonspecific indicator of metabolism that can be deranged for a variety of reasons (e.g., ischemia or inflammation) and may be irrelevant or only indirectly related to any AD-related process in certain individuals.

The PET tracer N - methyl[^{11}C]2 - (4' - methylaminophenyl) - 6 - hydroxy - benzothiazole, better known as Pittsburgh compound B (^{11}C-PIB), has been used to detect amyloid deposition *in vivo*. Previous ^{11}C-PIB PET studies reported quantitative increases in ^{11}C-PIB uptake, reflecting greater amyloid burden, in AD and MCI patients compared with controls [7-10]. In AD, ^{11}C - PIB uptake is particularly evident in the frontal, parietotemporal, and posterior cingulate cortices, consistent with the known distribution of amyloid plaques [11-13]. Less work has been done with ^{11}C-PIB in patients with MCI, which is associated with an increased likelihood of converting to AD. ^{11}C - PIB studies in small samples suggested that approximately two-thirds of patients with amnestic MCI (aMCI) show ^{11}C - PIB retention similar to AD, whereas one-third of patients are within the healthy control range [7-8, 14-16]. In MCI, amyloid - positive ^{11}C - PIB PET may indicate an increased likelihood of converting to AD [17].

The most common genetic variant associated with late-onset AD is apolipoprotein E (*ApoE*) *ε4* allele [18-19]. The presence of the *ε4* allele confers a significantly higher likelihood of developing AD. *ApoE* genotypes are also associated with AD biomarkers, with the presence of the *ApoEε4* allele associated with greater amyloid deposition [20 - 22] and alterations in brain function and glucose metabolism [23 - 25] in patients with MCI and AD and cognitively healthy older adults.

The present study investigated the relationship between plaque deposition and glucose metabolism using ^{11}C-PIB PET and ^{18}F-FDG PET in AD and aMCI patients and assessed the presence of the *ApoEε4* allele to explore the correlation between aMCI and AD.

Methods

Subjects

A total of 14 AD patients and 10 aMCI patients were randomly recruited at Tianjin Huanhu Hospital, Tianjin, China, between April 2012 and October 2012. All of the subjects underwent an extensive diagnosis and behavioral assessment by trained neurologists. The diagnosis of AD was made according to the criteria of National Institute of Neurological and Communicative Disorders and Stroke and the Alzheimer's Disease and Related Disorders Association (NINCDS-ADRDA) [26]. The diagnosis of dementia was

based on the criteria of Diagnostic and Statistical Manual of Mental Disorders, 4th edition (DSM-Ⅳ)[27]. No familial cases of AD were included in this study. To avoid the inclusion of vascular dementia cases, we excluded patients who scored > 2 points on the Hachinski Ischemic Scale[28]. Amnestic MCI was diagnosed using Petersen criteria[29], which require subjective memory complaints and serial reaction time scores for either immediate or delayed recall > 1.50 standard deviation (SD) below age - and education-adjusted norms in the absence of impairment in activities of daily living.

All of the controls were required to have a Mini-Mental State Examination (MMSE) score ⩾ 28, serial reaction time total and delayed recall scores within 1 SD of age-adjusted norms, and no current diagnosis of any DSM-Ⅳ Axis Ⅰ psychiatric disorder, neurological disorder or acute medical illness. A family history of dementia was not an exclusion criterion. Subjects who received Warfarin or had any contraindication to undergoing MRI or PET were excluded from the study. Controls were group-matched to patients with regard to age and sex.

MRI

MR images were acquired using a 3.0T Siemens Trio a Tim MR scanner. Coronal T_1WI was acquired using a three-dimensional spoiled gradient recalledecho (3D-SPGR) sequence [repetition time (TR) = 11 ms, echo time (TE) = 4.94 ms, flip angle (FA) = 20°, 1 mm slice thickness (zero gap), 160 slices, field of view (FOV) = 230 mm × 230 mm]. All of the images were reconstructed to a size of 256 × 256 with an isotropic resolution of 1 mm × 1 mm × 1 mm.

PET imaging

Head movement was minimized using a polyurethane immobilizer molded around the head. The PET images were acquired on a GE Discovery LS PET/CT scanner in the three-dimensional scanning mode, yielding 35 slices with 4.25 mm thickness that covered the entire brain. ^{11}C-PIB PET scans were acquired during 90-min dynamic PET acquisition (a total of 34 frames: 4 × 15 s, 8 × 30 s, 9 × 60 s, 2 × 180 s, 8 × 300 s, 3 × 600 s). ^{11}C-PIB was administered into an antecubital vein as a bolus injection, with a mean dose of 370-555 MBq. Then those images were reconstructed to a 128 × 128 matrix (2.50 mm × 2.50 mm pixel size).

The ^{18}F-FDG study was conducted 1 h after the ^{11}C-PIB PET scan using the same scanner, scanning mode, positioning and reconstruction matrix. The subjects received an intravenous injection of 250 MBq ^{18}F-FDG and remained in a darkened, quiet room. A 10-min static PET emission scan was performed 60 min after the ^{18}F-FDG injection.

A. Quantification of ^{11}C-PIB uptake

The uptake of ^{11}C-PIB was quantified at the voxel level using the region-to-cerebellum ratio, which was identical to the standardized uptake value ratio (SUVR). This simplified quantification enabled the utilization of a short 30-min image acquisition.

B. Automated region-of-interest analysis

Standardized region of interest (ROI) were defined on the MRI template image that represented brain anatomy in accordance with the Montreal Neurological Institute (MNI). We merged and pooled subsets from the original Automated Anatomic Labeling (AAL) atlas to form the following ROIs: middle frontal gyrus (MFG), medial prefrontal cortex (MPFC), lateral temporal cortex (LTC), hippocampus and parahippocampus (HF +), inferior parietal lobe (IP), posterior cingulate cortex and precuneus (PCCPre), striatum, thalamus, occipital lobe (OL), superior temporal gyrus (STG), and supplementary motor area (SMA).

C. Image preprocessing

The preprocessing of the ^{11}C-PIB imaging data was performed using Statistical Parametric Mapping 8 (SPM8) software and MATLAB 2010b for Windows (Mathworks, Natick, MA, USA). First, ^{11}C-PIB integral images (data corrected for radioactive decay summed from 60 to 90 min post-injection) were created from the dynamic PET images (frames 32 to 34) and coregistered to the subject's MR images. Second, the MR images were segmented into three classes (gray matter, white matter and cerebrospinal fluid) in SPM8 using 16 non-linear iterations and 7 × 9 × 7 basis functions. Third, the PET images and gray matter MR images were normalized using a T_1-weighted MRI template that was delivered with SPM to obtain normalization parameters. The application of a 0.50 threshold to the gray matter probability map created a gray matter probability map in MNI space. The gray matter probability map was then coregistered to the AAL template, and the PET counts were extracted from the gray matter probability map and ROIs. The mean values for all of the regions were calculated from the integral ^{11}C-PIB image. Target-to-cerebellum ratios were subsequently calculated for 11 bilateral regions.

D. ^{18}F-FDG PET image and statistical analysis

Spatial preprocessing and statistical analyses of ^{18}F-FDG PET images in all of the subjects were also performed using SPM8 software and MATLAB 2010b for Windows. We compared cerebral glucose metabolism

in the AD group with the control group. We also compared cerebral glucose metabolism between each aMCI subject and the control group. First, ^{18}F-FDG PET images were converted to ANALYZE format and then normalized to the MNI standard proportional stereotaxic space. Second, an isotropic 10 mm full-width half-maximum Gaussian spatial smoothing filter was applied to the image. Third, all of the comparisons of brain metabolism were performed on a voxel-by-voxel basis using a two-sample *t*-test. Statistical significance was determined using an extent threshold of 50 voxels. Regions that reached an uncorrected *P* value of less than 0.001 were considered statistically significant.

ApoE genotyping

Genomic DNA was extracted from total blood, and the *ApoE* gene was amplified by polymerase chain reaction (PCR) using reaction conditions modified from Wenham et al [32]. The two primers were 5'-TCCAAGGAG-GTGCAGGCGGCGCA-3' (upstream) and 5'-ACAGAATTCGCC-CCGGCCTGGTACACTGCCA-3' (downstream). Briefly, each amplification contained 200 ng of genomic DNA, 25 pmol of primer, 2.50 μl of 10% dimethyl sulfoxide, and 0.50 units of Taq DNA polymerase in a final volume of 25 μl. In the thermal reactor, initial denaturation occurred at 94 ℃ for 5 min, followed by 40 cycles of denaturation at 94 ℃ for 1 min, annealing at 65℃ for 1 min, extension at 72 ℃ for 1 min, and final extension at 72 ℃ for 10 min. The amplification product (20 μl) was then digested with 5 units Cfo1 for at least 3 h at 37 ℃. The samples were then subjected to electrophoresis for 2 h at 200 V on 12% native polyacrylamide gel. The genotypes were determined by the size of the DNA fragments present, viewed, and photographed under ultraviolet light after staining with 0.5 μg/ml ethidium bromide. We determined all of the genotypes without knowledge of the patient-control status.

Follow-up

The subjects with aMCI were clinically followed for 1-1.50 years after their baseline ^{11}C-PIB PET scan. During this follow-up period, no change was found in their diagnosis, and they still fulfilled the criteria for MCI (nonconverters), or their symptoms and clinical performance declined to the extent that they fulfilled the NINCDS-ADRDA criteria [19] for a diagnosis of probable AD (converters).

Statistical analyses

Descriptive statistics were used to make comparisons on the demographic and clinical variables for the 3 groups of subjects (control, aMCI and AD) and the ^{11}C-PIB+aMCI and ^{11}C-PIB-aMCI subgroups. Independent Student's *t*-tests were used to determine the differences in the ^{11}C-PIB SUVR and ^{18}F-FDG SPM between the AD group and control group. Analysis of variance (ANOVA) was used to compare differences in radiotracer uptake within the different brain regions among 4 groups (AD, ^{11}C-PIB+aMCI, ^{11}C-PIB-aMCI and control). Significant main effects in the ANOVA were followed by two-tailed *t*-tests for *post hoc* pairwise comparisons. Values of $P < 0.05$ were considered statistically significant.

Table 1. Demographic and cognitive characteristics of subjects in 3 groups

Observation item	Control (N = 5)	aMCI (N = 10)	AD (N = 14)
Sex case (%)			
Male	2 (2/5)	5 (5/10)	7 (7/14)
Female	3 (3/5)	5 (5/10)	7 (7/14)
Age ($\bar{x} \pm s$, year)	62.10 ± 11.00	65.80 ± 9.82	64.20 ± 10.61
Education ($\bar{x} \pm s$, year)	13.00 ± 3.51	12.20 ± 4.01	12.10 ± 3.34
Duration ($\bar{x} \pm s$, year)		1.60 ± 2.09	3.70 ± 2.02
C-MMSE ($\bar{x} \pm s$, score)	28.80 ± 1.34	26.20 ± 1.94	12.80 ± 6.64
MoCA ($\bar{x} \pm s$, score)	27.30 ± 2.11	21.10 ± 4.40	6.75 ± 4.65
ADL ($\bar{x} \pm s$, score)	20.00 ± 0.00	21.30 ± 2.05	42.60 ± 15.41
CDR ($\bar{x} \pm s$, score)	0	0.50 ± 0.31	1.40 ± 0.52
ApoEε4 carrier case (%)	0 (0/5)	3 (3/10)	5 (5/14)

C-MMSE, Chinese Mini-Mental State Examination (range 0–30); MoCA, Montreal Cognitive Assessment; ADL, Activities of Daily Living; CDR, Clinical Dementia Rating Scale

Ethics

Detailed informed written consent was obtained from all subjects and their relatives. The study was approved by Tianjin Huanhu Hospital and Tianjin Medical University Ethics Committees. The procedures were done in accordance with the ethical standards of Committee on Human Experimentation of Tianjin Huanhu Hospital and Tianjin Medical University.

Results

Clinical data

The control, aMCI and AD groups were compared with each other regarding to demographic and cognitive characteristics of subjects in each group (Table 1). These subjects in 3 groups differed in cognitive performance on MMSE and Montreal Cognitive Assessment (MoCA), in which AD patients scored

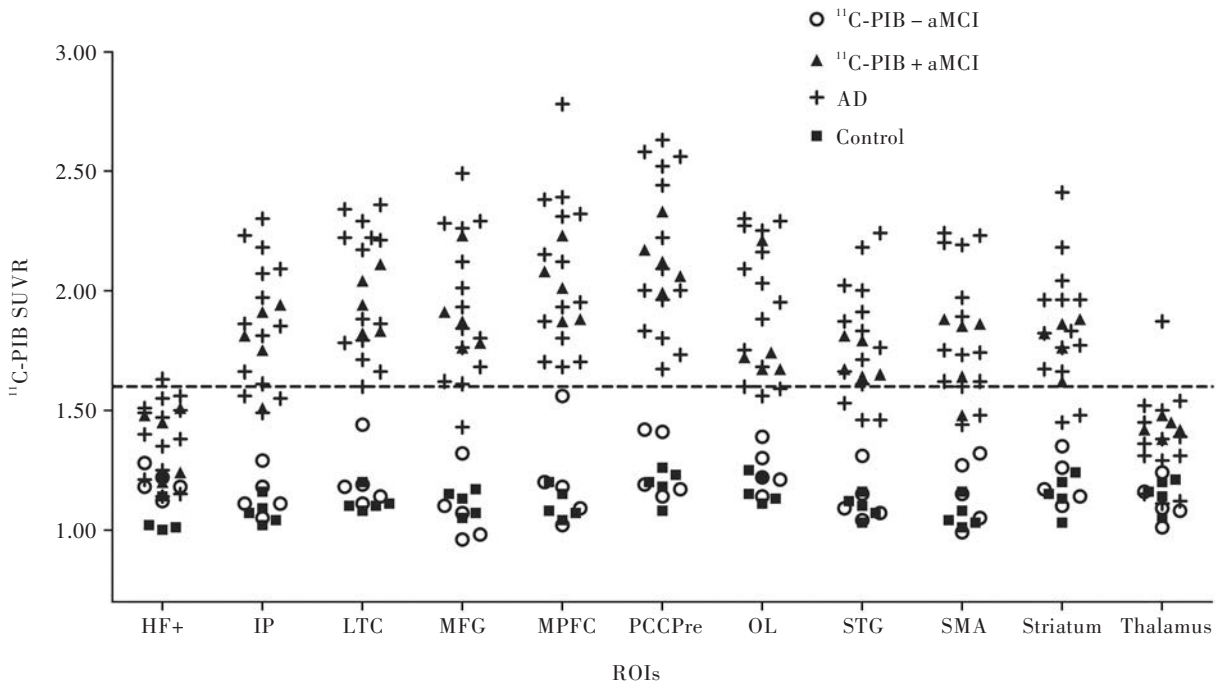

^{11}C-PIB, Pittsburgh compound B; aMCI, amnestic mild cognitive impairment; AD, Alzheimer's disease; SUVR, standardized uptake value ratio; ROIs, regions of interest; HF+, hippocampus and parahippocampus; IP, inferior parietal lobe; LTC, lateral temporal cortex; MFG, middle frontal gyrus; MPFC, medial prefrontal cortex; PCCPre, posterior cingulate cortex and precuneus; OL, occipital lobe; STG, superior temporal gyrus; SMA, supplementary motor area

Figure 1 Mean ^{11}C-PIB SUVRs in the AD, ^{11}C-PIB + aMCI, ^{11}C-PIB – aMCI, and control groups. Cases above the dashed line (SUVR = 1.60) had ^{11}C-PIB-positive scans. The scatter plots show individual region-to-cerebellum ratios over 60–90 min of the automated ROI analysis in the 11 ROIs in patients with AD, patients with aMCI and control subjects.

worse than MCI patients, and MCI patients scored worse than normal control subjects. The Activities of Daily Living (ADL) score was significantly higher in AD subjects than that in control and MCI subjects ($P < 0.05$), but the ADL score did not differ between the MCI and control groups.

^{11}C-PIB PET

Voxel-based automatic quantitative analysis was used to determine the mean ^{11}C-PIB SUVR in AD, ^{11}C-PIB + aMCI, ^{11}C-PIB- aMCI, and control groups (Figure 1). The mean ^{11}C-PIB SUVR was higher in the IP, LTC, MFG, MPFG, PCCPre, OL, SMA, and striatum in the AD group than in control group (range, 1.80-2.10 and 1.10-1.20; $P < 0.05$). ^{11}C-PIB binding levels in the aMCI group were bimodal. Using 1.60 as a negative cutoff value for ^{11}C-PIB, the aMCI group could be divided into ^{11}C-PIB + aMCI (N = 5) and ^{11}C-PIB- aMCI (N = 5) subgroups. No significant difference in the ^{11}C-PIB SUVR was found between the ^{11}C-PIB + aMCI subgroup and AD group ($P > 0.05$) or between the ^{11}C-PIB- aMCI subgroup and control group ($P > 0.05$) in all of the ROIs (Figure 2).

^{18}F-FDG PET

^{18}F-FDG SPM showed hypometabolism in the bilateral IP, posterolateral portions of the temporal lobe, PCCPre, and frontal lobe in AD subjects. In aMCI subjects, hypometabolism was relatively mild compared with the AD group. Three of 5 ^{11}C-PIB + aMCI subjects exhibited hypometabolism in the bilateral parietal lobes, lateral temporal cortex, and PCCPre. Three of 5 ^{11}C-PIB- aMCI subjects exhibited hypometabolism in the bilateral frontal lobes and anterior cingulate cortex. The remaining 4 subjects had normal ^{18}F-FDG PET (Figure 3).

Regional analyses of ^{11}C-PIB and ^{18}F-FDG

The SPM and ROI analyses showed Aβ deposition and hypometabolism in the same regions in the AD group. In the ^{11}C-PIB + aMCI group, high Aβ deposition and ^{18}F-FDG hypometabolism were consistently found in parietal regions, including the PCCPre, and lateral temporal cortex, but inconsistency was observed in the frontal lobe, with high amyloid deposition but

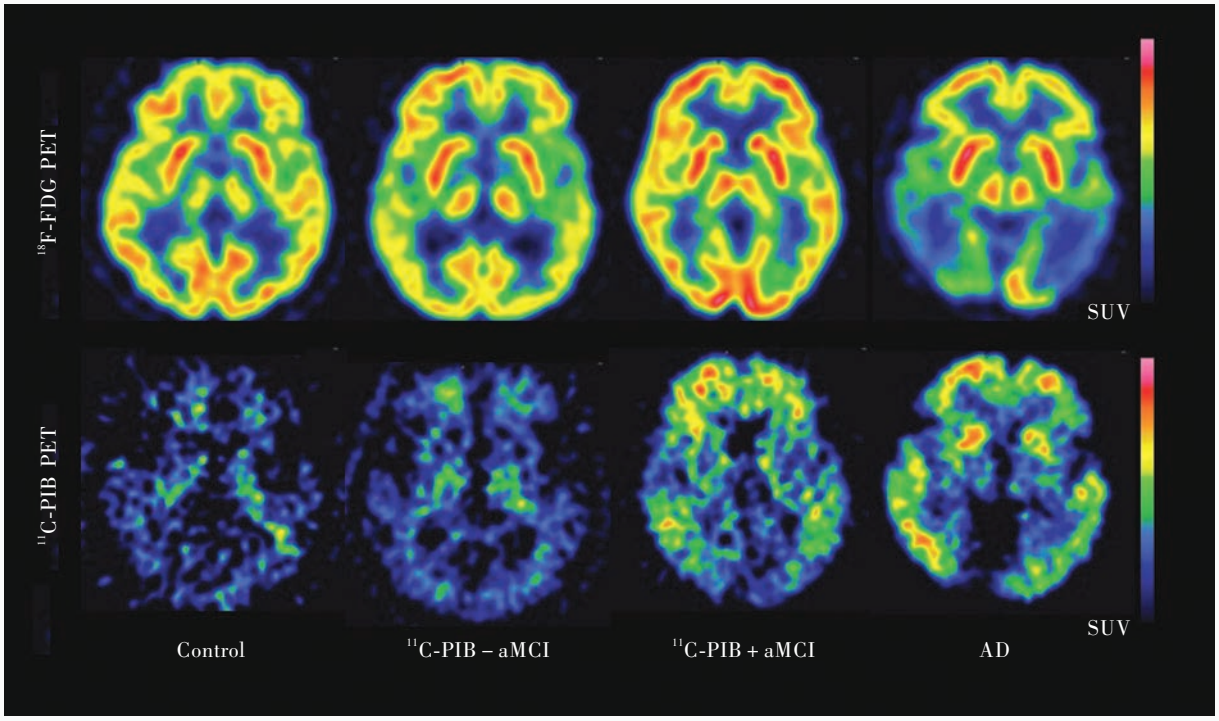

^{11}C-PIB, Pittsburgh compound B; ^{18}F-FDG, ^{18}F-fluorodeoxyglucose; PET, positron-emission tomography; aMCI, amnestic mild cognitive impairment; AD, Alzheimer's disease; SUV, standardized uptake value

Figure 2 Examples of axial ^{18}F-FDG and ^{11}C-PIB SUV images for control, ^{11}C-PIB – aMCI, ^{11}C-PIB + aMCI and AD subjects.

preserved ^{18}F-FDG metabolism.

Comparison between ^{11}C - PIB + aMCI and ^{11}C-PIB - aMCI subgroups

The ^{11}C-PIB + aMCI and ^{11}C-PIB - aMCI subgroups were not different with regard to age, age at onset, gender, and education (Table 2). Although the mean MMSE and MoCA scores were higher in the aMCI - subgroup than in the aMCI + subgroup, no statistically significant difference was observed. The ratio of *ApoE ε 4* allele carriers was higher in the ^{11}C - PIB + aMCI group (3/5) than in the ^{11}C-PIB - aMCI group (0/5, $P < 0.01$).

Follow-up in aMCI group

During a 12-18 month follow - up period after their baseline ^{11}C - PIB PET scans, 2 of the 10 subjects with aMCI (20%) clinically converted to AD. Both of these converters were ^{11}C - PIB - positive, with bilateral parietal lobes, lateral temporal cortex, and PCCPre hypometabolism at baseline, making the percentage conversion rate in the ^{11}C - PIB + aMCI subgroup 40% over this same follow-up period. Two converters were *ApoE ε 4* carriers. One ^{11}C - PIB - aMCI subject with bilateral frontal lobes and anterior cingulate cortex hypometabolism converted to FTD.

Discussion

The ^{11}C-PIB SUVR was > 1.60 and higher in the IP, LTC, MFG, MPFG, PCCPre, OL, SMA and striatum in AD patients compared with the control group but not in the hippocampal region, which is consistent with the literature [7, 10, 30]. These findings support the relative regional distribution of Aβ deposition reported in other ^{11}C - PIB studies that also found increased prefrontal, parietal, and precuneus uptake [7, 10]. The results are also consistent with autopsy data that showed that Aβ deposition in early AD is greater in the frontal and parietal cortices than in the hippocampus [31]. ^{11}C - PIB binding levels in the aMCI group were variable and bimodal. Based on the cutoff value used in the present study, 50% of the MCI patients had low ^{11}C - PIB binding rates, similar to controls, and 50% exhibited no differences with AD patients in all of the ROIs. One possible explanation for these data is that ^{11}C-PIB - MCI subjects who have been followed in the clinic for more than 1 year without converting to AD dementia would be less likely to have AD brain pathology than MCI patients who are ^{11}C - PIB - positive in the initial evaluation.

Control subjects with high ^{11}C - PIB retention were not present in our sample. In contrast, a previous

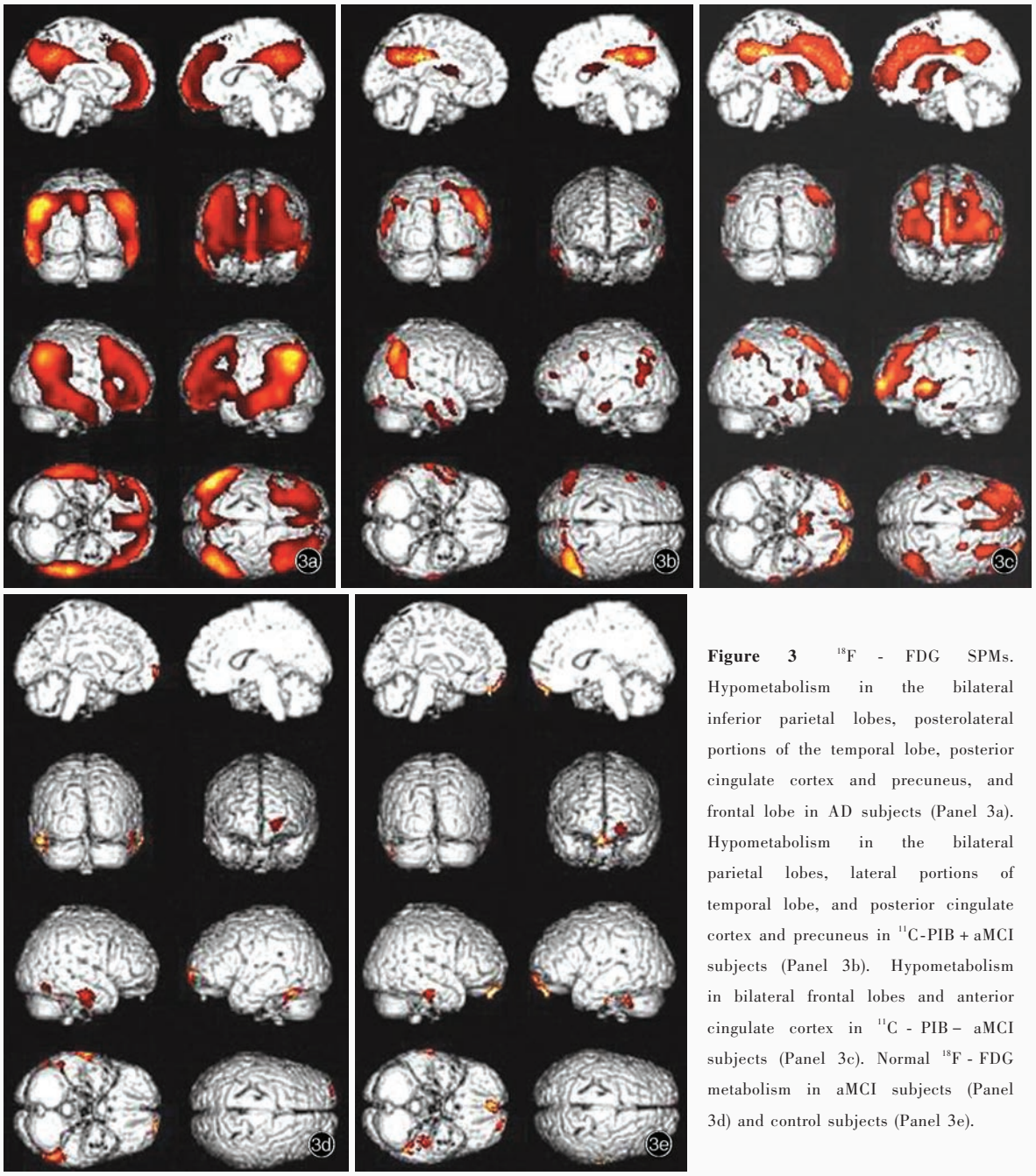

Figure 3 ^{18}F - FDG SPMs. Hypometabolism in the bilateral inferior parietal lobes, posterolateral portions of the temporal lobe, posterior cingulate cortex and precuneus, and frontal lobe in AD subjects (Panel 3a). Hypometabolism in the bilateral parietal lobes, lateral portions of temporal lobe, and posterior cingulate cortex and precuneus in ^{11}C-PIB + aMCI subjects (Panel 3b). Hypometabolism in bilateral frontal lobes and anterior cingulate cortex in ^{11}C - PIB – aMCI subjects (Panel 3c). Normal ^{18}F - FDG metabolism in aMCI subjects (Panel 3d) and control subjects (Panel 3e).

study reported high ^{11}C-PIB retention in approximately 20% of healthy elderly control subjects [22]. Different criteria used to select control subjects may partly account for these differences across studies. In the present study, impairment on neuropsychological tests was a strict exclusion criterion for healthy control subjects, in contrast to the use of CDR of global cognitive/functional ability in some studies, which may have allowed for the inclusion of control subjects with mild neuropsychological deficits [32]. Importantly, the present study had relatively small control samples and the age of the control less than 65 years.

Initial follow-up studies suggested that increased ^{11}C - PIB retention is associated with an increased likelihood that healthy controls will convert to MCI and MCI patients will convert to AD [16, 33]. In a recent study, ^{11}C - PIB - positive patients with MCI were more likely to convert to AD than ^{11}C-PIB-negative patients, and faster converters had higher ^{11}C - PIB retention levels at baseline than slower converters [17]. In patients diagnosed with AD, no increase [34] or a small increase in ^{11}C-PIB retention may be found during the follow-up

Table 2. Comparison of clinical data between 2 aMCI subgroups

Observation item	aMCI+ (N=5)	aMCI− (N=5)	*P* value
Sex case (%)			0.500
Male	2 (2/5)	3 (3/5)	
Female	3 (3/5)	2 (2/5)	
Age ($\bar{x}\pm s$, year)	62.80±6.01	64.40±10.38	0.773
Age at onset ($\bar{x}\pm s$, year)	60.40±5.54	62.40±10.71	0.721
Duration ($\bar{x}\pm s$, year)	2.40±1.14	2.20± 0.45	0.724
Education ($\bar{x}\pm s$, year)	8.20±1.04	11.20± 2.77	0.080
MMSE ($\bar{x}\pm s$, score)	24.80±1.31	26.40± 1.51	0.111
MoCA ($\bar{x}\pm s$, score)	18.20±3.40	22.00± 5.19	0.117
Visuospatial/executive ($\bar{x}\pm s$, score)	2.80±1.09	4.40± 1.34	0.073
Attention ($\bar{x}\pm s$, score)	5.60±0.89	5.20± 1.30	0.222
Delayed recall ($\bar{x}\pm s$, score)	1.40±1.34	1.40± 1.34	1.000
Naming ($\bar{x}\pm s$, score)	2.60±0.54	2.80± 0.44	0.545
Language ($\bar{x}\pm s$, score)	1.40±0.89	2.00± 1.22	0.402
Abstraction ($\bar{x}\pm s$, score)	0.80±0.84	1.00± 1.00	0.740
Orientation ($\bar{x}\pm s$, score)	3.60±1.14	5.20± 1.30	0.073
ADL ($\bar{x}\pm s$, score)	22.40±2.30	20.40± 0.89	0.108
ApoEε4 carrier case (%)	3 (3/5)	0 (0/5)	0.000

MMSE, Mini-Mental State Examination; ADL, Activities of Daily Living

peroid [14, 35-36]. These results indicate that once the stage of established AD is reached, Aβ deposition in most regions has plateaued. In our ^{11}C-PIB-positive aMCI subgroup, the ^{11}C-PIB SUVRs were consistent with AD in the frontal, parietal and occipital lobes. One possibility is that Aβ deposition plateaued in these regions, and these patients may be more likely to convert to AD. At the 1-year follow-up, the MMSE and MoCA scores declined significantly in 2 ^{11}C-PIB-positive aMCI patients, who converted to the clinical AD stage.

^{18}F-FDG hypometabolism differed between the AD and control groups in bilateral PCCPre, IP, posterolateral portions of the temporal lobe and frontal lobe but not in the hippocampus or parahippocampal gyrus. These findings are consistent with the literature on metabolic deficits in the parietal and posterior cingulate that distinguish AD from control subjects [3]. In this sample, however, no significant differences were found in medial temporal regions. Some other reports indicated that metabolic deficits in both the parietal and temporal lobes distinguish AD from control subjects [37]. Metabolic deficits in AD gradually worsen throughout the course of the disease. More advanced stages of the disease usually involve prefrontal association areas, and primary cortices may eventually be affected. Six of our AD subjects were already in the moderate stage of the disease with frontal lobe involvement. Three of 5 ^{11}C-PIB-positive aMCI subjects exhibited hypometabolism in the bilateral parietal lobe, lateral temporal cortex, and PCCPre. Previous ^{18}F-FDG PET studies that used small samples of MCI patients reported that hypometabolism in the parietotemporal and posterior cingulate may characterize future converters to AD [5-6]. These ^{11}C-PIB-positive patients with hypometabolism may have a greater probability of converting to AD dementia. Another study that used a small sample suggested that regional decreases in the regional cerebral metabolic rate of glucose in the parietal and posterior cingulate may be superior to ^{11}C-PIB in distinguishing MCI from control subjects [38]. In our sample, however, 3 of 5 ^{11}C-PIB-aMCI subjects exhibited hypometabolism in the bilateral frontal lobes and anterior cingulate but not in the parietal and posterior cingulate. These patterns of hypometabolism are consistent with FTD [4]. In our 1-year follow-up, one of the subjects converted to FTD. One possibility is that these patients would convert to FTD or another dementia but not AD dementia. However, this needs to be clarified in longitudinal studies.

In our aMCI group, the ^{11}C-PIB-positive subgroup had more *ApoEε4* carriers than the ^{11}C-PIB-negative subgroup and control group, consistent with previous studies that suggested that the presence of the *ApoEε4* allele is associated with increased ^{11}C-PIB retention in AD [20, 39]. Postmortem studies have reported correlations between the presence of the *ApoEε4* allele and higher Aβ burden in the brains of patients with sporadic AD [40-41]. Okello et al [17] found an association between *ApoEε4* status in PIB-positive subjects with MCI and the rate of clinical conversion to AD, and all of the faster converters were *ApoEε4* carriers. In the present study, two ^{11}C-PIB+aMCI converted patients were *ApoEε4* carriers, also suggesting that the *ApoEε4* allele accelerated the conversion from aMCI to AD.

One limitation of the present study was its cross-sectional design. Follow-up data to examine the prognostic implications of the baseline PET findings are clearly needed. The sample size in the present study was also relatively small. A study with a larger patient sample would be of great interest to determine the aMCI patterns that are more likely to convert to AD dementia.

Conclusion

^{11}C-PIB PET is a powerful tool to screen aMCI with AD pathology. The aMCI patients with AD pathology in the present study who exhibited hypometabolism in the parietal lobe, lateral temporal cortex and precuneus in ^{18}F-FDG PET and were *ApoEε4* allele carriers were more likely to convert to clinical AD dementia. These PET techniques combined with *ApoE* genotyping

provide complementary information to strongly distinguish diagnostic groups in cross - sectional comparisons, but longitudinal studies are still required.

Acknowledgements

This study was supported by Tianjin Science and Technology Support Programs (No. 12ZCZDSY02900, 12ZCZDSY01600), Science and Technology Project of Tianjin Municipal Health Bureau (No. 11KG117) and Natural Science Foundation of Tianjin (No. 13JCYBJC21300).

Disclosure

No authors report any conflict of interest.

References

[1] Selkoe DJ. Alzheimer´s disease: genotypes, phenotypes, and treatments. Science, 1997, 275:630-631.

[2] Mirra SS, Heyman A, McKeel D, Sumi SM, Crain BJ, Brownlee LM, Vogel FS, Hughes JP, van Belle G, Berg L. The Consortium to Establish a Registry for Alzheimer´s Disease (CERAD). Part Ⅱ. Standardization of the neuropathologic assessment of Alzheimer´s disease. Neurology, 1991, 41:479 - 486.

[3] Minoshima S, Giordani BJ, Berent S, Frey KA, Foster NL, Kuhl DE. Metabolic reduction in the posterior cingulate cortex in very early Alzheimer´s disease. Ann Neurol, 1997, 42:85-94.

[4] Ishii K, Sakamoto S, Sasaki M, Kitagaki H, Yamaji S, Hashimoto M, Imamura T, Shimomura T, Hirono N, Mori E. Cerebral glucose metabolism in patients with frontotemporal dementia. J Nucl Med, 1998, 39:1875-1878.

[5] Chételat G, Desgranges B, de la Sayette V, Viader F, Eustache F, Baron JC. Mild cognitive impairment: can FDG-PET predict who is to rapidly convert to Alzheimer´s disease? Neurology, 2003, 60:1374-1377.

[6] Drzezga A, Lautenschlager N, Siebner H, Riemenschneider M, Willoch F, Minoshima S, Schwaiger M, Kurz A. Cerebral metabolic changes accompanying conversion of mild cognitive impairment into Alzheimer´s disease: a PET follow - up study. Eur J Nucl Med Mol Imaging, 2003, 30:1104-1113.

[7] Rowe CC, Ng S, Ackermann U, Gong SJ, Pike K, Savage G, Cowie TF, Dickinson KL, Maruff P, Darby D, Smith C, Woodward M, Merory J, Tochon-Danguy H, O´Keefe G, Klunk WE, Mathis CA, Price JC, Masters CL, Villemagne VL. Imaging beta - amyloid burden in aging and dementia. Neurology, 2007, 68:1718-1725.

[8] Kemppainen NM, Aalto S, Wilson IA, Någren K, Helin S, Brück A, Oikonen V, Kailajärvi M, Scheinin M, Viitanen M, Parkkola R, Rinne JO. PET amyloid ligand [11C]PIB uptake is increased in mild cognitive impairment. Neurology, 2007, 68: 1603-1606.

[9] Verhoeff NP, Wilson AA, Takeshita S, Trop L, Hussey D, Singh K, Kung HF, Kung MP, Houle S. In-vivo imaging of Alzheimer disease beta - amyloid with [11C]SB - 13 PET. Am J Geriatr Psychiatry, 2004, 12:584-595.

[10] Klunk WE, Engler H, Nordberg A, Wang Y, Blomqvist G, Holt DP, Bergström M, Savitcheva I, Huang GF, Estrada S, Ausén B, Debnath ML, Barletta J, Price JC, Sandell J, Lopresti BJ, Wall A, Koivisto P, Antoni G, Mathis CA, Långström B. Imaging brain amyloid in Alzheimer´s disease with Pittsburgh Compound-B. Ann Neurol, 2004, 55:306-319.

[11] Delacourte A, David JP, Sergeant N, Buée L, Wattez A, Vermersch P, Ghozali F, Fallet-Bianco C, Pasquier F, Lebert F, Petit H, Di Menza C. The biochemical pathway of neurofibrillary degeneration in aging and Alzheimer´s disease. Neurology, 1999, 52:1158-1165.

[12] Morris JC, Storandt M, McKeel DW Jr, Rubin EH, Price JL, Grant EA, Berg L. Cerebral amyloid deposition and diffuse plaques in "normal" aging: evidence for presymptomatic and very mild Alzheimer´s disease. Neurology, 1996, 46:707-719.

[13] Thal DR, Rüb U, Orantes M, Braak H. Phases of Abeta - deposition in the human brain and its relevance for the development of AD. Neurology, 2002, 58:1791-1800.

[14] Forsberg A, Engler H, Almkvist O, Blomquist G, Hagman G, Wall A, Ringheim A, Långström B, Nordberg A. PET imaging of amyloid deposition in patients with mild cognitive impairment. Neurobiol Aging, 2008, 29:1456-1465.

[15] Jack CR Jr, Lowe VJ, Senjem ML, Weigand SD, Kemp BJ, Shiung MM, Knopman DS, Boeve BF, Klunk WE, Mathis CA, Petersen RC. 11C PiB and structural MRI provide complementary information in imaging of Alzheimer´s disease and amnestic mild cognitive impairment. Brain, 2008, 131:665-680.

[16] Wolk DA, Price JC, Saxton JA, Snitz BE, James JA, Lopez OL, Aizenstein HJ, Cohen AD, Weissfeld LA, Mathis CA, Klunk WE, De - Kosky ST. Amyloid imaging in mild cognitive impairment subtypes. Ann Neurol, 2009, 65:557-568.

[17] Okello A, Koivunen J, Edison P, Archer HA, Turkheimer FE, Någren K, Bullock R, Walker Z, Kennedy A, Fox NC, Rossor MN, Rinne JO, Brooks DJ. Conversion of amyloid positive and negative MCI to AD over 3 years: an 11C - PIB PET study. Neurology, 2009, 73:754-760.

[18] Corder EH, Saunders AM, Strittmatter WJ, Schmechel DE, Gaskell PC, Small GW, Roses AD, Haines JL, Pericak-Vance MA. Gene dose of apolipoprotein E type4 allele and the risk of Alzheimer´s disease in late onset families. Science, 1993, 261: 921-923.

[19] Bertram L, Lill CM, Tanzi RE. The genetics of Alzheimer disease: back to the future. Neuron, 2010, 68:270-281.

[20] Drzezga A, Grimmer T, Henriksen G, Mühlau M, Perneczky R, Miederer I, Praus C, Sorg C, Wohlschläger A, Riemenschneider M, Wester HJ, Foerstl H, Schwaiger M, Kurz A. Effect of APOE genotype on amyloid plaque load and gray matter volume in Alzheimer disease. Neurology, 2009, 72:1487-1494.

[21] Morris JC, Roe CM, Xiong C, Fagan AM, Goate AM, Holtzman DM, Mintun MA. APOE predicts amyloid - beta but not tau Alzheimer pathology in cognitively normal aging. Ann Neurol, 67:122-131.

[22] Fleisher AS, Chen K, Liu X, Roontiva A, Thiyyagura P, Ayutyanont N, Joshi AD, Clark CM, Mintun MA, Pontecorvo MJ, Doraiswamy PM, Johnson KA, Skovronsky DM, Reiman EM. Using positron emission tomography and florbetapir F18 to image cortical amyloid in patients with mild cognitive impairment or dementia due to Alzheimer disease. Arch Neurol, 2011, 68:1404-1411.

[23] Bookheimer SY, Strojwas MH, Cohen MS, Saunders AM, Pericak-Vance MA, Mazziotta JC, Small GW. Patterns of brain activation in people at risk for Alzheimer´s disease. N Engl J Med, 2000, 343:450-456.

[24] Bondi MW, Houston WS, Eyler LT, Brown GG. fMRI evidence of compensatory mechanisms in older adults at genetic risk for

Alzheimer disease. Neurology, 2005, 64:501-508.
[25] Langbaum JB, Chen K, Lee W, Reschke C, Bandy D, Fleisher AS, Alexander GE, Foster NL, Weiner MW, Koeppe RA, Jagust WJ, Reiman EM; Alzheimer's Disease Neuroimaging Initiative. Categorical and correlational analyses of baseline fluorodeoxyglucose positron emission tomography images from the Alzheimer's Disease Neuroimaging Initiative (ADNI). Neuroimage, 2009, 45:1107-1116.
[26] McKhann G, Drachman D, Folstein M, Katzman R, Price D, Stadlan EM. Clinical diagnosis of Alzheimer's disease: report of the NINCDS - ADRDA Work Group under the auspices of Department of Health and Human Services Task Force on Alzheimer's Disease. Neurology, 1984, 34:939-944.
[27] American Psychiatric Association. Diagnostic and statistical manual of mental disorders. 4th ed. Washington DC: American Psychiatric Association, 2000: 157-158.
[28] Rosen WE, Terry RD, Fuld PA, Katzman R, Peck A. Pathological verification of ischemic score in differentiation of dementias. Ann Neurol, 1980, 8:486-488.
[29] Petersen RC, Doody R, Kurz A, Mohs RC, Morris JC, Rabins PV, Ritchie K, Rossor M, Thal L, Winblad B. Current concepts in mild cognitive impairment. Arch Neurol, 2001, 58:1985-1992.
[30] Ng S, Villemagne VL, Berlangieri S, Lee ST, Cherk M, Gong SJ, Ackermann U, Saunder T, Tochon - Danguy H, Jones G, Smith C, O'Keefe G, Masters CL, Rowe CC. Visual assessment versus quantitative assessment of 11C - PIB PET and 18F - FDG PET for detection of Alzheimer's disease. J Nucl Med, 2007, 48: 547-552.
[31] Price JL, Morris JC. Tangles and plaques in nondemented aging and "preclinical" Alzheimer's disease. Ann Neurol, 1999, 45: 358-368.
[32] Mintun MA, Larossa GN, Sheline YI, Dence CS, Lee SY, Mach RH, Klunk WE, Mathis CA, DeKosky ST, Morris JC. [11C]PIB in a nondemented population: potential antecedent marker of Alzheimer disease. Neurology, 2006, 67:446-452.
[33] Villemagne VL, Pike KE, Darby D, Maruff P, Savage G, Ng S, Ackermann U, Cowie TF, Currie J, Chan SG, Jones G, Tochon-Danguy H, O'Keefe G, Masters CL, Rowe CC. Abeta deposits in older non - demented individuals with cognitive decline are indicative of preclinical Alzheimer's disease. Neuropsychologia, 2008, 46:1688-1697.
[34] Engler H, Forsberg A, Almkvist O, Blomquist G, Larsson E, Savitcheva I, Wall A, Ringheim A, Långström B, Nordberg A. Two - year follow - up of amyloid deposition in patients with Alzheimer's disease. Brain, 2006, 129:2856-2866.
[35] Edison P, Archer HA, Hinz R, Hammers A, Pavese N, Tai YF, Hotton G, Cutler D, Fox N, Kennedy A, Rossor M, Brooks DJ. Amyloid, hypometabolism, and cognition in Alzheimer disease: an [11C]PIB and [18F]FDG PET study. Neurology, 2007, 68:501-508.
[36] Jack CR Jr, Lowe VJ, Weigand SD, Wiste HJ, Senjem ML, Knopman DS, Shiung MM, Gunter JL, Boeve BF, Kemp BJ, Weiner M, Petersen RC; Alzheimer's Disease Neuroimaging Initiative. Serial PIB and MRI in normal, mild cognitive impairment and Alzheimer's disease: implications for sequence of pathological events in Alzheimer's disease. Brain, 2009, 132: 1355-1365.
[37] Silverman DH, Small GW, Chang CY, Lu CS, Kung De Aburto MA, Chen W, Czernin J, Rapoport SI, Pietrini P, Alexander GE, Schapiro MB, Jagust WJ, Hoffman JM, Welsh-Bohmer KA, Alavi A, Clark CM, Salmon E, de Leon MJ, Mielke R, Cummings JL, Kowell AP, Gambhir SS, Hoh CK, Phelps ME. Positron emission tomography in evaluation of dementia: regional brain metabolism and long-term outcome. JAMA, 2001, 286:2120-2127.
[38] Li Y, Rinne JO, Mosconi L, Pirraglia E, Rusinek H, DeSanti S, Kemppainen N, Någren K, Kim BC, Tsui W, de Leon MJ. Regional analysis of FDG and PIB-PET images in normal aging, mild cognitive impairment, and Alzheimer's disease. Eur J Nucl Med Mol Imaging, 2008, 35:2169-2181.
[39] Reiman EM, Chen K, Liu X, Bandy D, Yu M, Lee W, Ayutyanont N, Keppler J, Reeder SA, Langbaum JB, Alexander GE, Klunk WE, Mathis CA, Price JC, Aizenstein HJ, DeKosky ST, Caselli RJ. Fibrillar amyloid - beta burden in cognitively normal people at 3 levels of genetic risk for Alzheimer's disease. Proc Natl Acad Sci USA, 2009, 106:6820-6825.
[40] Schmechel DE, Saunders AM, Strittmatter WJ, Crain BJ, Hulette CM, Joo SH, Pericak - Vance MA, Goldgaber D, Roses AD. Increased amyloid beta - peptide deposition in cerebral cortex as a consequence of apolipoprotein E genotype in late-onset Alzheimer disease. Proc Natl Acad Sci USA, 1993, 90: 9649-9653.
[41] Rebeck GW, Reiter JS, Strickland DK, Hyman BT. Apolipoprotein E in sporadic Alzheimer's disease: allelic variation and receptor interactions. Neuron, 1993, 11:575-580.